

Stimulated nuclear polarization – a new method for studying the mechanisms of photochemical reactions

Renad Z. Sagdeev, Elena G. Bagryanskaya

Institute of Chemical Kinetics and Combustion,
Novosibirsk, 630090, USSR

Abstract – This report concerns a fundamentally new high-sensitive magnetic resonance method for detection of short-lived species – radical pairs, radical ion pairs, biradicals and radicals – the method of stimulated nuclear polarization (SNP). The SNP-method is based on the resonance mw-field effects on nuclear polarization in the products of the radical reactions. Using this method one can obtain information on the ESR spectrum of intermediate short-lived RP and on the channels of reaction product formation.

INTRODUCTION

Study of intermediate short-lived species particularly important to understand the elementary mechanisms of photochemical reactions. This report concerns a fundamentally new high-sensitive magnetic resonance method for detection of such species – the method of stimulated nuclear polarization (SNP). This method has considerable advantages over the well-known technique of chemically induced dynamic nuclear polarization (CIDNP) (ref. 1). The SNP method is based on the resonance mw field effect on the singlet-triplet conversion in radical pairs (RP) (refs. 2-4). Resonance mw field induces the S-T transitions in RP selective to the nuclear spin orientation, which leads to the formation of nuclear polarization in the products of these radical pairs. Analyzing the dependence of mw-field induced nuclear polarization on the value of external magnetic field, one can obtain information about the ESR spectrum of intermediate short-lived radical pairs and the channels of reaction product formation. The present report gives the short review of the main principles of the SNP method, and discusses a number of its applications to the solution of various photochemical problems.

PRINCIPLES OF THE METHOD

Consider the mechanism of SNP formation in a single-proton RP in high magnetic fields. Let us assume that the RP was formed in the triplet state and recombination from the triplet state is forbidden (in the general case, it is known that the singlet (S) and triplet (T) states have different probabilities (ref. 1)). In the case of high fields, hyperfine interaction (HFI) mixes effectively only the T_0 and S levels. CIDNP effect, as is generally known, is based on the fact that the S-T transition probabilities differ for RP with different nuclear spin orientations. Suppose now g -factors of the radicals to be equal. In this case, for a single-proton RP CIDNP equals to zero. The resonance mw-field mixes the T_0 state of the RP with T_+ and T_- states, which leads at low mw-field amplitudes $\omega_1 = \gamma_e B_1$:

$$\omega_1 < |\omega^a - \omega^b| \quad (1) \text{ to acceleration and at}$$

$$\omega_1 > |\omega^a - \omega^b| \quad (2) \text{ to deceleration of S-T conversion (refs. 4-6),}$$

here ω^a and ω^b are the frequencies of ESR transitions in the RP partners Ra(H) and Rb respectively. Let the condition (1) be fulfilled. If the resonance mw-field frequency equals ω_α^a – the frequency of ESR transitions with an α -orientation of nuclear spins, the acceleration of T-S transition will take place only in the subensemble of RP with the α -orientation of nuclear spins. Thus, RP recombination products will have mainly the nuclei with α -projection of nuclear spins, which will be reflected in enhanced absorption lines in the NMR spectrum of the products. The nuclei of escape RP products will be mainly with β -projection, their NMR signals being an emission lines.

If the mw-field frequency is equal to ω_β^a - the ESR frequency of an RP with β -orientation of nuclear spins, the NMR lines of the RP recombination products will show emission, the escape RP products exhibiting absorption. mw-field at the frequency ω_β^b will induce S-T conversion acceleration equal efficiency for both the RP subensembles and, hence, will not change the nuclear polarization of the RP products. When $\omega_1 > |\omega^a - \omega^b|$, i.e. under spin-locking conditions (refs. 4-6), mw-field retards the S-T conversion and, consequently, SNP signs will be opposite with respect to the abovementioned case.

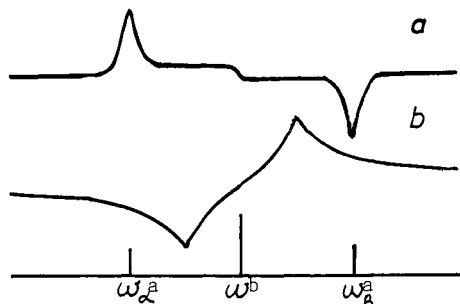


Fig. 1. The SNP observed ESR spectrum of one proton radical pair a) in the absence of spin-locking, $\omega_1 \ll a$; b) under the conditions of spin-locking, $\omega_1 > a$. The lines of the ESR spectrum of the model RP are shown schematically.

Proceeding from these qualitative considerations, one can formulate the following rule for the sign of the net SNP of a particular nucleus. The latter is determined by the sign of the product of the following quantities: $\Gamma = \mu \varepsilon a_k \psi \eta$. Here $\mu = 1$ for triplet, and $\mu = -1$ for singlet RP precursor, or $\varepsilon = -1$ for k -incage or escape product; a_k is the isotropic constant of HFI with the k -th nucleus whose polarization is under consideration. The value of ψ equals 1 or -1 when mw pumping is performed for low- or high-field HFS component, respectively, of chosen nucleus; a positive or negative value of η corresponds to pumping in the absence of k -spin-locking or in the presence of spin-locking. $\Gamma > 0$ refers to a positive SNP effect (A - absorption), $\Gamma < 0$ to negative SNP effect (E - emission).

EXPERIMENTAL

For experimental realization of the method it is necessary to perform pumping of electron resonance transitions in RP during photochemical reaction. Integration of a resonator or an oscillatory circuit with the probe of a commercial NMR spectrometer is a very difficult technical problem. In this respect it is more simple to perform the pumping and detection separately. Block diagram of the home-made setup (refs. 3,8) is shown in Fig. 2.

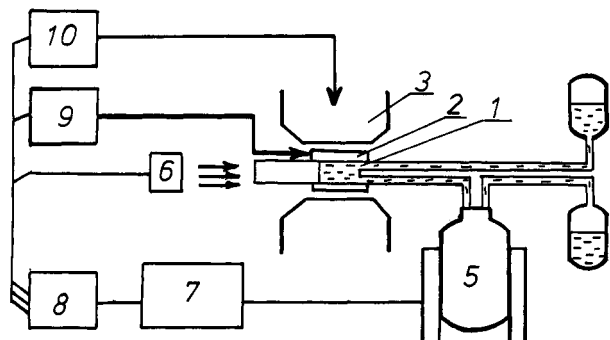


Fig. 2. Block diagram of the experimental apparatus, 1- photochemical cell; 2- cavity, or oscillatory circuit coil; 3- magnet; 4- flow system; 5- probe and solenoid of NMR spectrometer; 6- the laser or UV-lamp; 7- NMR-spectrometer; 8- programmer; 9- mw-generator; 10- magnet power supply.

The solution was UV-irradiated in a special cell (1) placed inside the resonator (2) in the field of auxiliary magnet (3) to make the direction of the constant magnetic field B_0 perpendicular to that of the mw-field B_1 . Then a flow system (4) transferred the sample to the probe of a Varian XL-200 NMR spectrometer (5) where the NMR spectra of reaction products were detected. A pulsed UV-laser (Lambda Physik, 150 mJ) and a high-pressure Hg-lamp DRSh-500 were used as light sources (6). The laser pulse duration was 15 ns, wavelength - 308 nm. Resonance transitions of RP were saturated at different frequencies $f = 100, 150, 310, 1530, 1590$ MHz. To synchronize the mw-field generator and laser with NMR-spectrometer operation, a home-made programmer was employed. Fig. 3a depicts schematically the time diagram of the experiment. The minimal step of the sweep of variable delay of mw-pulse

τ_d is 10 ns, the maximal is 75 μ s. The pulse duration τ_i can be incremented with either 75 or 300 ns step. The maximum mw-pulse duration is 30 μ s. This setup allows to realize two types of experiments to be realized. First, at fixed τ_i and τ_d one may study the dependence of the NMR signal intensity on the B_0 field and, second, at fixed B_0 one may vary τ_i and τ_d to obtain kinetic information. The time resolution of the pulsed experiment is determined by mw-pulse decay. We have succeeded in decreasing the decay length down to 30 ns with B_1 amplitude being equal to 0.3 mT.

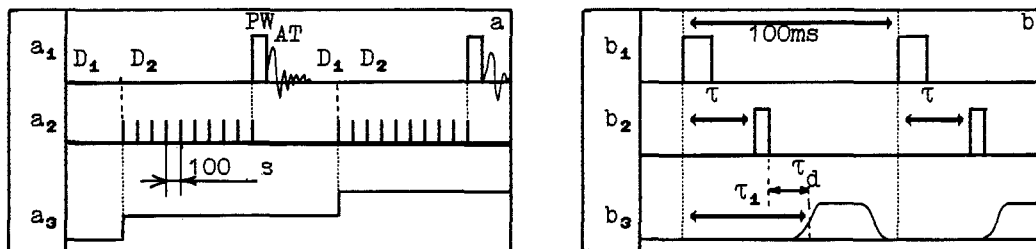


Fig. 3. (a) Time-diagram of the experiments on time resolved SNP. PW, AT-detection pulse and acquisition time of NMR spectra, D_1 - delay between the end of AT- interval and the following measurement cycle; D_2 - delay between the beginning of the recording cycle and pulse; a_1 -the pulse sequence S2PUL of the NMR spectrometer; a_2 -laser flashes; a_3 - the changes in the magnitude of the external magnetic field B_0 ; (b) Synchronization of laser and mw-generator. b_1 -laser triggering pulses; b_2 -laser flashes; b_3 - the pulses of mw field B_1 .

MODEL SYSTEMS

General mechanisms of SNP have been studied in photolytic reactions of parabenzoquinone and duroquinone in CD_3CN , $CDCl_3$, CD_3OD solutions. Characteristic changes in NMR spectra, caused by mw field effect are shown in Fig. 4 for the photolysis of parabenzoquinone in CD_3CN solution. It is seen from Fig. 4 that SNP effects can reach significant values. Figure 5 shows SNP spectrum (the dependence of the SNP effect, i.e. the difference in the NMR signal intensities during the pumping of electron transitions with mw-field B_1 and without it, on B_0) detected during the photolysis of duroquinone in CD_3OD . The spectrum corresponds to the durosemiquinone radical in RP.

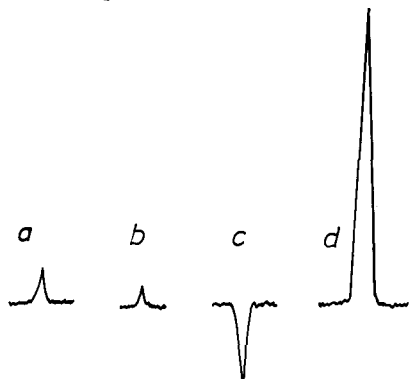


Fig. 4. NMR spectra of the photolysis of 10^{-3} M benzoquinone in acetonitrile in magnetic field $B_0=2.8$ mT; a) dark; b) under illumination; c) under illumination and during the pumping of electron transition at 100 MHz, $B_1=0.07$ mT; d) under illumination and mw-field $B_1=1.0$ mT.

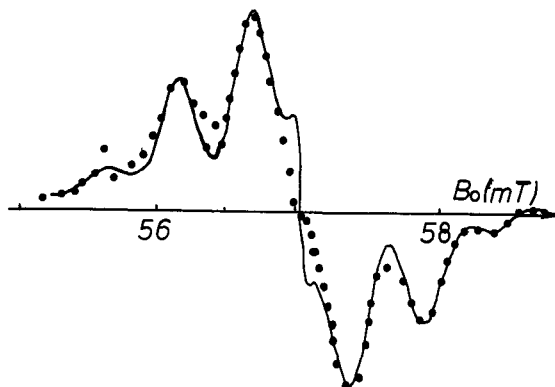


Fig. 5. Experimental SNP spectra detected by duroquinone NMR signal during photolysis of 10^{-3} M duroquinone in methanol, $B_1=0.1$ mT. Solid line shows calculated SNP spectrum of RP of two durosemiquinone radicals (ref. 7).

At small B_1 SNP spectrum, unlike RYDMR (refs. 5,10) spectra, changes insignificantly with changing the partner of the pair. Fig. 5 shows calculated SNP spectrum of the pair $DQH-DQH$. The calculations were performed by the method of summation of radical pair re-encounter contributions to the recombination of neutral radical in the framework of a continuous diffusion

model. The calculation technique have been described in detail by Mikhailov and co workers (ref. 4). The A/E type of the SNP spectrum detected by NMR lines of CH_3 -group indicates that the DQ is the cage product of triplet RP. Fig. 6 illustrates changes in SNP spectra with increasing mw-field amplitude B_1 on the photolysis of benzoquinone in CD_3CN . The spectrum observed corresponds to an RP of two semiquinone radicals. At $B_1=1.0$ mT the observed SNP spectrum is inverted due to spin-locking (refs. 5-7).

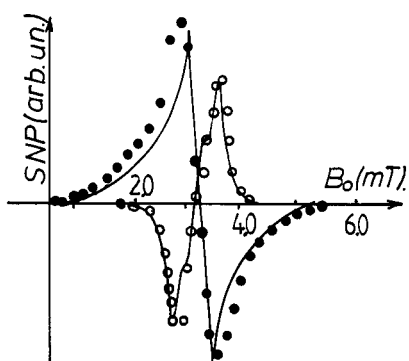


Fig. 6 SNP spectra detected for benzoquinone NMR signals for 10^{-3}M parabenzoquinone in acetonitrile during the photolysis (\bullet) $B_1=1.0$ mT; (\circ) $B_1=0.07$ mT. Solid lines shown the calculated SNP spectra for the RP of two semiquinone radicals. $f=100$ MHz. $a_{\text{meta}}=-5.09$ mT; $a_{\text{orto}}=0.29$ mT. $a_{\text{para}}=-.189$ mT (ref. 9).

IDENTIFICATION OF INTERMEDIATE RADICAL SPECIES

As was mentioned above, the SNP technique allows one to identify the intermediate short-lived species, RP and RIP, as well as yields an information about the channels of reaction product formation. SNP in combination with time-resolved CIDNP has been used for a complex study of elementary stages in the photolysis of anthraquinone (A) with triethylamine (TEA) in media with various polarities (ref. 11). SNP spectra detected by TEA CH_2 -groups signal during the photolysis of 10^{-2}M of TEA and $5 \cdot 10^{-4}\text{M}$ of AQ in acetonitrile are presented in Fig. 7a. These spectra correspond to TEA cation-radical in the RP (the constants of HFI for CH_2 -groups protons and nitrogen are equal to 2.16 mT (ref. 12)). From the type of the SNP spectrum (A/E) one may conclude that TEA is the incage product of RP.

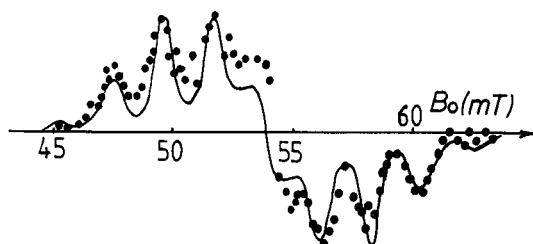


Fig. 7a. SNP spectrum detected for NMR signal of TEA CH_2 -group during the photolysis of $5 \cdot 10^{-4}\text{M}$ AQ and 10^{-2}M TEA in acetonitrile. Solid line is calculated SNP spectra of RP $\text{TEA}^+ - \text{AQ}$. $B_1=0.3$ mT; $f=1530$ MHz.

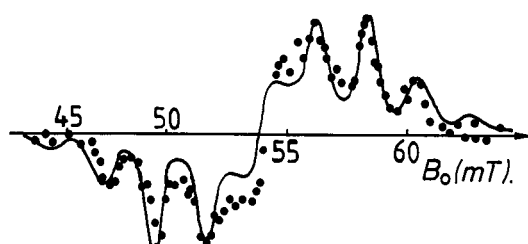
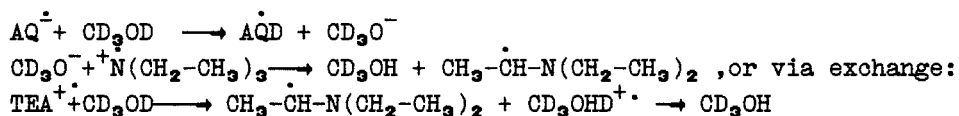


Fig. 7b. SNP spectrum detected for NMR signal of methanol OH-group during the photolysis of $5 \cdot 10^{-4}\text{M}$ AQ with 10^{-2}M TEA in metanol. Solid line is the same as in Fig. 7a. but for escape product.

The SNP spectra observed for NMR signal of TEA CH_2 -groups during the photolysis of AQ and TEA in CD_3OD and in acetonitrile are the same. Methanol OH group shows the SNP spectrum different from that registered for NMR signal of TEA only by sign (A/E) (Fig. 7b) and, hence, corresponding to the escape radical cation TEA^+ . This facts unambiguously point to the appearance of a hydroxyl proton in the alcohol from the CH_2 -group of the escape TEA cation radical. This in its turn suggests the presence of the following reactions:



In nonpolar solvents (benzene), the SNP spectrum corresponds to the ESR spectrum of aminalkyl radical $\text{CH}_3\text{-CH-N(Et)}_2$ in the RP ($a(\text{CH}_3)=1.958$ mT, $a(\text{N})=0.518$ mT, $a(\text{H})=-1.365$ mT (ref. 9), Fig. 8). The spectrum was detected from NMR signal of CH_3 -group protons. The spectrum sign (E/A) points to the escape formation of TEA in this reaction. Time-resolved CIDNP results for this reaction are in good agreement with the abovementioned data.

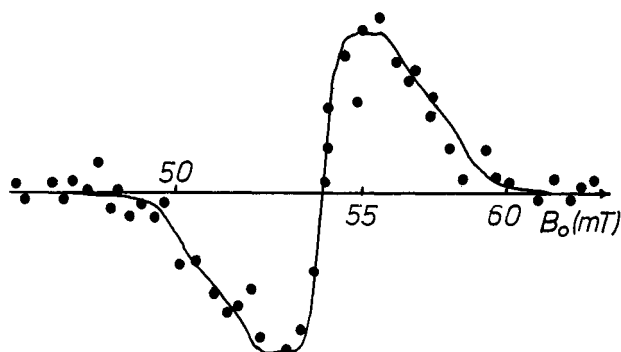


Fig. 8. SNP spectrum detected for NMR signal of CH_3 -group of TEA during the photolysis of AQ with TEA in benzene. Solid line is calculated SNP spectrum of RP $\text{AQH}\cdot\text{CH-N(Et)}_2$; $B_1=0.6$ mT.

DEGENERATE ELECTRON EXCHANGE REACTIONS

SNP. Degenerate electron exchange has a substantial influence on SNP spectra. However, the use of the method to obtain charge transfer rate constants is complicated by the fact that the exchange between spectral components with different signs results in total decrease in SNP signal amplitude, and at a rapid exchange - in disappearance of the signal. The main peculiarities of the exchange exhibition in SNP spectra are considered elsewhere (ref. 14).

DNP. Analyzing some radical-ion reactions accompanied by degenerate electron exchange (photolysis of anthracene (Ac) with dimethylaniline (DMA), Ac with diethylaniline, photolysis of fumaronitrile (FN) in the presence of naphthalene (Naph), etc. (refs. 13,14)), in low magnetic fields, we observed, besides the SNP effects, the dynamic nuclear polarization (DNP) of a significant value. The main characteristic properties of the DNP effect in these reactions are the following.

1. The effect is observed only in low magnetic fields, in high fields the effect is absent.
 2. The sign of the observed polarization is the same for all the ESR spectrum components and is independent of nuclear spin projections (unlike the SNP spectrum sign) and of cross-relaxation mechanism in radical (unlike the sign of ordinary DNP (ref. 15,3)).
 3. Changes in the concentration of the reactant entering into the charge transfer reaction cause exchange narrowing of the spectrum.
- Proceeding from these properties, we propose the following model for DNP formation in low magnetic fields due to electron exchange. As is generally known, charge transfer causes modulation of electron interaction with nuclei, which leads to phase and population relaxations of nuclear spins with formation of longitudinal and transverse relaxation times T_1 and T_2 (ref. 16):

$$1/T_1 = \Delta^2 \tau_e (1 + 1/\omega^2 \tau_e^2) ; \quad 1/T_2 = 2\Delta^2 \tau_e / (1 + \omega^2 \tau_e^2) \quad (3)$$

where Δ^2 is the second moment of the HFS spectrum of the radical, determined via the i -th nucleus spin value I_i and the HFS constant a_i as follows $\Delta^2 = \sum I_i(I_i+1)a_i^2/3$ (ω is Larmor precession of electron spin, τ_e - the charge transfer time, $\tau_e = 1/KC$, where K is the charge transfer rate constant and C is the concentration of molecules). It is seen from exprs(3) that in high fields $\omega\tau_e \gg 1$ only the transverse relaxation is substantial which is formed in the high fields due to the secular part of the electron-nuclear interaction which does not result in electronic and nuclear spin flips. However, in sufficiently low fields $\omega\tau_e < 1$, the longitudinal relaxation induced by electron and nuclear spin flip-flop transitions, becomes significant. Two variants are possible: (i) the radicals have nonequilibrium population of the electron levels due to CIDEP effects. Since the longitudinal relaxation occurs only due to flip-flop transitions, the disappearance of the electron polarization is accompanied by formation of the nuclear polarization equal to the electron one, i.e. the transfer of CIDEP to CIDNP takes place. Switching on the resonance mw-field leads to decay and, in the saturation point of ESR transitions, to disappearance of CIDNP and thus, to decrease in the nuclear polarization transferred from the electron one. The sign of the nuclear

polarization in this case is determined by the sign of CIDEP.

(ii) CIDEP in radicals is absent. In this case, saturating the transitions the mw-field creates nonequilibrium electron polarization which is transferred to nuclear polarization due to cross relaxation. Highly important is the fact that during radical-ion lifetime the electron polarization is transferred to a number of diamagnetic molecules participating in the electron exchange. The polarization lifetime in these molecules reaches several seconds, and thus the polarization is accumulated. Hence, unlike the ordinary Overhauser effect, the enhancement coefficient in this case can be significantly larger than the limiting enhancement coefficient of DNP $\gamma_e \beta / \gamma_n \beta_n$. Theoretical description of this effect is given elsewhere (ref. 13). Here we shall present only final expression for the intensity of the nuclear polarization due to the effect described above:

$$I(\omega) = \frac{T^*}{T_1} \cdot \frac{\omega_1^2 T_1^* T_2^*}{(1 + \Delta\omega T_1^* T_2^* + \omega_1^2 T_1^* T_2^*)} \cdot (\langle S_z(0) \rangle + \langle S_0 \rangle \tau_r / T_1) \quad (4)$$

where T_r is the total radical lifetime, $\langle S_z(0) \rangle$ is the initial electron polarization; $\langle S_0 \rangle$ is the equilibrium Boltzmann electron polarization in the field B_0 . Fig. 9a demonstrates experimental DNP spectra obtained on photolysis of anthracene (Ac) with dimethylaniline (DMA) in acetonitrile. The same figure shows the curves calculated by formula (4).

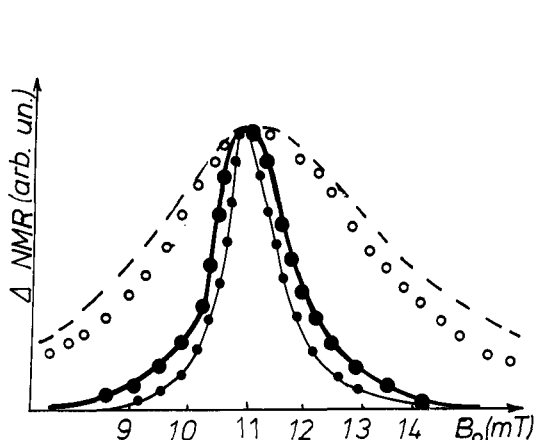


Fig. 9a. DNP spectra detected for NMR signal of the phenyl-group of DMA during photolysis of $5 \cdot 10^{-4}$ M anthracene with DMA (○) - 10^{-4} M; (●) - 0.5 M; (●) - 1 M; $B_1 = 0.3$ mT.

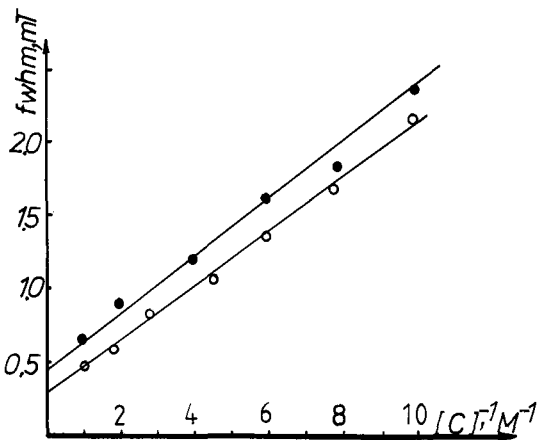
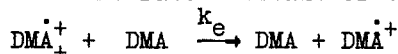


Fig. 9b. The dependence of DNP spectrum fwhm on the reverse concentration of the DMA. $f = 310$ MHz; (○) - $B_1 = 0.3$ mT; (●) - $B_1 = 0.45$ mT.

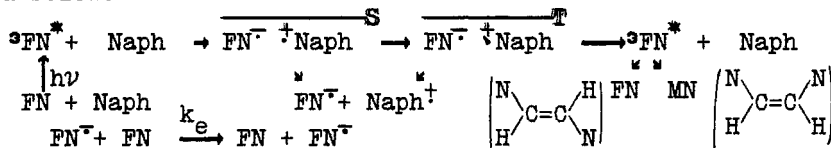
The abovementioned effect in combination with SNP may be applied to solution of various problems, obtaining electron exchange rates, identification of intermediate radical species, studying the reaction mechanism. Studying the dependence of DNP spectrum fwhm on the reverse concentration of the reagent participating in the degenerate electron exchange reaction, one can obtain the electron exchange rate constants (Figs. 9a, 9b). Thus, we have obtained the rate constant of the reaction:



equal to $3.4 - 0.3 \cdot 10^{11}$ / M s. The SNP and DNP techniques have been used for the investigation of the photolytic reaction mechanism of a number of aromatic azines (phenazine, acridine, dibenzphenazine, 4-2-N-N-dimethylaminophenazine) with DMA. The DNP spectra of DMA radical cations have been detected for all the azines studied except for the phenazine, that indicates the radical-ion pathway of the reaction. No DNP effect was observed in photolysis of phenazine with DMA in acetonitrile. Moreover, the SNP spectrum corresponding to phenazine radical in the RP has been detected. The sign of the spectrum shows that the reaction occurs from the excited triplet state. The ESR spectrum detected in this reaction corresponds to phenazine radical.

Application of the SNP and DNP methods to analysis of reactions of fumaronitrile with naphthalene in acetonitrile has confirmed the mechanism of photosensitized *cis-trans*-isomerization of fumaronitrile assumed earlier

(ref. 16) on the basis of CIDNP effects. The scheme of the reaction is presented below:



The SNP spectra (Fig. 10a) show that fumaronitrile is principally formed from singlet RP and maleonitrile - from triplet pair, which is consistent with early results (ref. 16). In going to low magnetic fields, fumaronitrile protons show significant DNP effect (Fig. 10b, 10c) while maleonitrile shows no DNP signal. This unambiguously points to the fact that photoisomerization takes place in the triplet molecule FN^* and not in the radical-ion FN or in RP. The electron exchange rate constant estimated by the exchange narrowing of the spectrum is 10^9 l/M s.

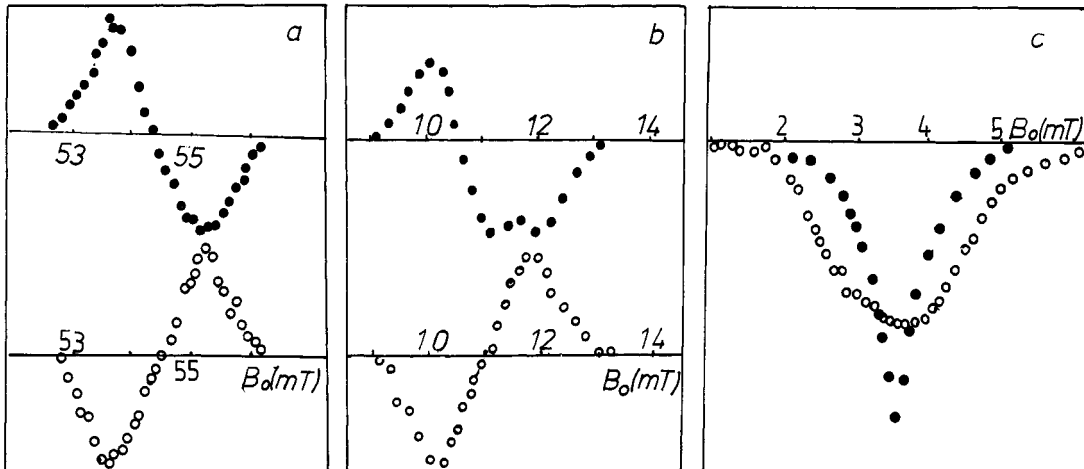


Fig. 10. SNP spectra detected for NMR signal of (●)-FN and (○)-MN during the photolysis of 0.01 M FN with $5 \cdot 10^{-3}$ M Naph in acetonitrile; a) $f=1530$ MHz, $B_1=0.25$ mT; b) $f=310$ MHz, $B_1=0.25$ mT; c) $f=100$ MHz, $B_1=0.1$ mT, (●)-0.1 M FN; (○)- 10^{-3} M FN.

RADICAL PAIRS WITH NONZERO EXCHANGE INTERACTION

The exchange electron spin-spin interaction is the magnetic interaction whose contribution to intersystem crossing of RP or biradicals is difficult to determine. Although it is obvious that in systems with relatively small separation of radical centers, e.g. in biradicals and RP localized in micelles, these interactions can play quite an important role. Certainly, the most direct experimental way of solving these problems is to obtain ESR spectra of corresponding systems. Since SNP, as well as RYDMR, is sensitive solely to RP products and reflects the mw-field effect only directly on singlet-triplet conversion in RP, it may be successfully applied to solution of the abovementioned problems. Let us consider how the exchange interaction exhibits itself in SNP spectra. Energy level diagram of an RP with one HFI constant (A), on the assumption of effective exchange interaction averaged over radical trajectories \bar{J} , is shown in Fig. 11. Relative location of energy levels are determined by relationships of the values A, \bar{J} , and external magnetic field B_0 . The effects of nuclear polarization, both chemically induced and stimulated, are essentially dependent on the relationship of intersystem crossing (ISC) rates $K(T_0-S)$, $K(T-S)$. When the average exchange interaction $2\bar{J} > B_0$, the rate of the ISC by the $T-S$ channel is higher than the rates of ISC crossing by other channels (T_0-S , T_+-S) ($K_{S-T} = V_{STi}^2 / (V_{STi}^2 + (\Delta E_i)^2)$ where ΔE_i is the energy gap between the S and T_i (T_0, T_+) states. In this case, the T_0 state population is less than that of the T_0, T_+ states. mw-field pumps up the T_0 level, enhancing the emission. SNP spectrum in this case differs substantially from the RP-SNP spectrum at $J=0$ and is an emissive line (Fig. 11a). In the other case, $K_{T_0-S} > K_{T-S}$, corresponding to the case when exchange interaction is less than the Zeeman splitting (Fig. 11b.) the T_0 state population is lower than that of T_0, T_+ states. Mw-field, in this case, will increase the number of biradicals decaying via the T-S interconversion. The SNP spectrum is an ordinary one, with the signs of spectral line polarization depend on the signs of nuclear spin projections.

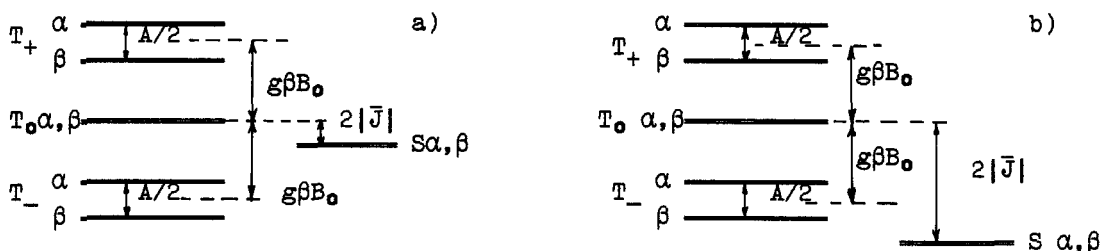
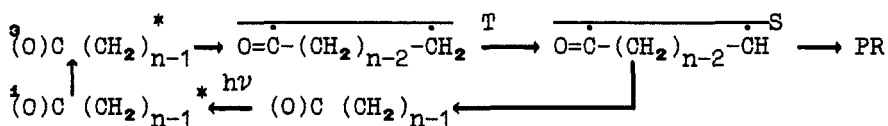


Fig. 11. Energy level diagram of an RP with non-zero exchange interaction $2\bar{J}$ and one magnetic nucleus ($A > 0$). T, S are the electron spin wavefunction; α, β are the nuclear spin states. a) $2|\bar{J}| < g\beta B_0$; b) $2|\bar{J}| > g\beta B_0$.

The presence of the exchange interaction in this case should be reflected by changed splittings in the spectrum (the line position is determined, as for an ordinary ESR spectrum (ref. 18), by the relationship of HFI and exchange interaction constants). SNP spectrum line intensities being different from those of an ESR spectrum by the dependence on nuclear spin projection and on recombination rate in a certain electron-nuclear state). The alternate exchange interaction exhibits itself in the broadening of SNP spectrum components.

Biradicals The SNP method has been employed in order to study the intermediate short-lived biradicals arising in the photolysis of some aliphatic cyclic ketones $(O)C(CH_2)_{n-1}$ for $n=10-13$ (refs. 19,20). The main route of the photolytic reaction of cycloalkanones is the α -cleavage of excited triplet ketones to yield acyl-alkyl biradicals (ref. 21):



Variation of ketone polymethylene chain length, HFI constants (by use of the ketones with deuterium- and CH_3 -group-substituted protons in α -position), external magnetic field B_0 (30, 110, 55 mT), as well as ^1H and ^{13}C detection of SNP, allowed us to change the relations of A, \bar{J}, B over a wide range. Figs. 12a,b,c,d show changes in SNP spectra of the biradicals with variation of exchange interaction, external field, and HFI constants. The results obtained are in good agreement with the abovementioned model on the assumption of the average exchange interaction \bar{J} . The estimated values of the average exchange interaction are consistent with the values obtained from the maxima of field dependences of CIDNP (ref. 22).

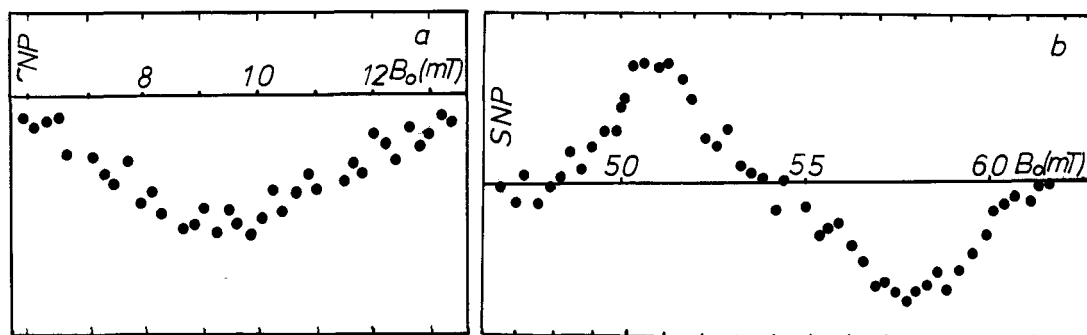
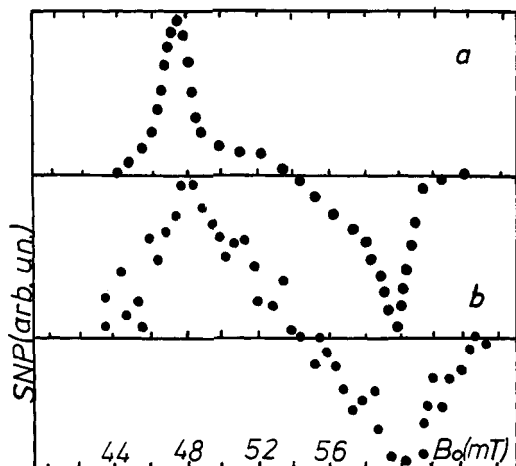


Fig. 12. a) SNP spectrum obtained for NMR line intensity of the ^{13}C α -carbon of cyclododecanone - d_4 during the pumping electron transition at 308 MHz, $B_1=1.0\text{mT}$, ($2\bar{J} > g\beta B_0$); b) SNP spectrum obtained from NMR line intensity of carbon $\gamma 1$ ^{13}C of cyclododecanone, $f=1530$ MHz, $B_1=0.3$ mT, ($2\bar{J} < g\beta B_0$).

RP in micelles SNP was used to study the RP localized in micelles during the photolysis of dibenzylketone (DBK) and α -methyldeoxybenzoin (MDB) in SDS micelles (ref. 23). In the photolysis of DBK an RP arises consisting of a benzyl and a phenylacetyl radicals, the lifetime of this pair being limited by decarbonylation of the phenylacetyl radical $k=6.4 \cdot 10^6$ 1/s (ref.24). Fig.13. shows SNP spectrum detected in this reaction by carbonyl carbon atom of DBK.



radical	A(^{13}C)(mT)	A(^{13}C)(mT)	A(^{13}C)(mT)
PhCH ₂ ^{13}C (O)	12.3 \pm 0.1	12.38(ref.24)	
Ph ^{13}C (O)	12.4 \pm 0.3	12.8 (ref.25)	
HC-CH HC ^{13}C -C(O) HC-CH	5.6 \pm 0.3	-	

Table 1. ^{13}C HFI constants measured by SNP.

Fig. 13. a) SNP spectra detected for NMR signal of carbonyl carbon of dibenzylketone NMR signal, during the photolysis of 10^{-3}M DBK in 0.1 M SDS in D_2O , $B_1=0.2$ mT, $f=1530$ MHz; (natural abundance of ^{13}C). b) the same as a) in benzene; $B_1=0.6$ mT; (45% enrichment ^{13}C).

Increased RP lifetime in micelles, compared to that in homogeneous solutions, leads to significantly increased (by hundreds of times) SNP signal. Hence, it is possible to study SNP in samples with the natural abundance of ^{13}C . During the investigation of MDB photolysis, SNP spectra have been detected for both carbonyl and α -phenyl carbon atom of MDB. Table 1 lists ^{13}C HFI constants measured by the SNP spectra in comparison with the reported ESR data on hfi constants of isolated radicals. As seen from the table, these values coincide within the measurement error. The coincidence between the hfi constants of isolated radicals and the same radicals being the partners of an RP indicates that exchange interaction in micelles is small and does not exceed the error of the measurement of hfi constants from SNP spectra, i.e. 0.1–0.4 mT.

TIME-RESOLVED SNP

The main difference between the pulsed and continuous variants of the SNP technique consists in the fact that the latter implies that RP (as well as intermediate short-lived radicals), during all their lifetimes, are affected by the mw-field B_1 inducing the S-T conversion in the RP or producing dynamic nuclear polarization (DNP) whilst the former provides the radically new possibility of the selective effect of the mw-field on RP subensembles (or radicals) with certain lifetimes.

Hence, the pulsed variant has some advantages:

- (i) the increased resolution of the method (in the continuous variant, even at decreased B_1 amplitude the contribution from the short-lived RP broadening the spectrum due to their lifetime remains)
- (ii) separation of geminate and diffusion pairs (studying SNP at various τ_d).
- (iii) separation of SNP and DNP contributions to the mw-induced nuclear polarization in radical reaction products
- (iv) a possibility to get unique information on RP and radical distribution by lifetimes (from SNP and DNP dependence on τ_d).

To demonstrate experimentally the potentialities and advantages of the pulsed SNP technique, we have chosen, as a model system, the photolysis of benzoyl peroxide in solution (CD_3OD , CD_3CN). This reaction is interesting because the intermediate RP contains an active phenyl radical which under standard conditions in liquid cannot be observed by the conventional ESR technique. Fig. 14 shows SNP spectrum measured from benzene NMR signal in the 50.0 mT field, $f=1530$ MHz. The photolysis of benzoyl peroxide is known to produce the singlet radical pair $\text{PhC}(O)\text{O}\cdot\text{Ph}$. The SNP spectrum phase (A/E) corresponds to the escape product of the singlet RP with account the positive sign of the constant of HFI in the phenyl radical. The SNP spectrum observed by NMR signal from the cage product - phenylbenzoate - is of the opposite sign (E/A). The asymmetry of the spectrum is due to large difference in g-factors of acyl and phenyl radicals (2.0093 and 2.002, respectively (ref. 12), $g=0.0073$, $\Delta g\beta B_0=0.39$ mT.).

Indeed, theoretical calculation of SNP spectrum in the field $B_0=54.5$ mT is in good agreement with experimental data (see Fig. 14). At $\tau_d=50$ ns we have succeeded in observation of an SNP spectrum considerably different from the corresponding spectrum at $\tau_d=0$ (Fig. 14). The spectrum observed ($\tau_d=80$ ns) is symmetrical and has the opposite pattern (E/A). We have studied SNP dependences on τ in various magnetic fields at various resonance lines.

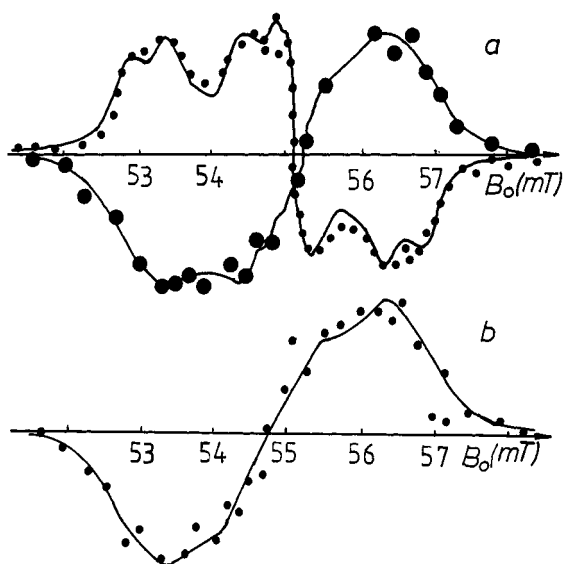


Fig. 14. a) SNP spectrum during benzoyl peroxide photolysis in CD_3OD detected for the (○)-benzene, $B_1=0.2$ mT; (●)-phenylbenzoate NMR signal, $B_1=0.6$ mT; $A=1.75$ mT, $A=0.62$ mT, $A=0.2$ mT. $f=1530$ MHz, $\tau_d=0$. b) the same as in a) measured for the benzene NMR signal, $\tau_d=100$ ns.

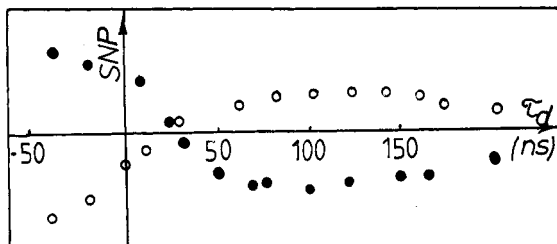


Fig. 15. The dependence of SNP intensity on τ_d , $B_1=0.6$ mT, (●) $B_0=52.8$ mT; (○) $B_0=56.35$ mT.

It has turned out that the spectrum inversion (from A/E to E/A) occurs at 50 ns and then changes insignificantly up to $\tau_d=200$ ns. The spectrum phase (E/A) indicates that the observed SNP spectrum^d corresponds to either the cage product of the singlet pair (which is impossible for benzene) or the escape product of the triplet F pair. The relative symmetry of the observed spectrum points to the absence of a marked Δg in the RP. The time range (50–200 ns), wherein the inverted (E/A) SNP spectrum was observed, is a characteristic of the diffusion F-pairs, such as Ph Ph or Ph CD_3OD .

CONCLUSION

The material considered shows the SNP technique to be a very powerful and informative method for investigation of photochemical reactions. This technique allows one to detect ESR spectra of intermediate short-lived radical species with very short lifetimes (to nanoseconds) as well as obtain structural and kinetic information. We think this method may be recommended for a wide use in practice.

REFERENCES

1. K.M. Salikhov, Yu.N. Molin, R.Z. Sagdeev and A.L. Buchachenko, in *Spin Polarization and Magnetic Effects in radical reaction*, ed. Yu.N. Molin (Elsevier, Amsterdam, 1984).
2. E.G. Bagryanskaya, Yu.A. Grishin et al., *Chem. Phys. Lett.*, **114**, 138-142 (1985).
3. E.G. Bagryanskaya et al., *Chem. Phys. Lett.*, **128**, 162-167 (1986).
4. S.A. Mikhailov, K.M. Salikhov, M. Plato, *Chem. Phys.*, **117**, 197-217 (1987).
5. S.I. Kubarev, E.A. Pshenichnov et al., *Chem. Phys. Lett.*, **73**, 370-380 (1980).
6. E.G. Bagryanskaya et al., *Chem. Phys. Lett.*, **128**, 417-419 (1986).
7. E.G. Bagryanskaya et al., *Chem. Phys. Lett.*, **117**, 220-223 (1985).
8. N.I. Avdievitch et al., *Chem. Phys. Lett.*, **155**, 141-145 (1989).
9. H. Fischer and K.H. Hellwege, eds. *Landolt-Bornstein, New Series, Group 2*, vol.9 (Springer, Berlin, 1977).
10. O.A. Anisimov, Yu.N. Molin, *J. Indust. Irrad. Technol.*, **2**, 271-290 (1984).
11. Yu.P. Tsentalovich, E.G. Bagryanskaya, *Chem. Phys.* (1990) in press.
12. V. M. Grigoriants, O.A. Anisimov et al., *Z. Strukt. Khim.*, **23**, 4-10 (1982).
13. E.G. Bagryanskaya, N.N. Lukzen et al., *Chem. Phys.*, (1990), in press.
14. K.H. Hausser and P. Stehlik, *Advan. Magn. Reson.*, **3**, 79-139 (1968).
15. A. Abragam, *The Principles of Nuclear Magnetism*, Clarendon Press, Oxford, 1961.
16. A.I. Kruppa, T.V. Leshina et al., *Chem. Phys. Lett.*, **121**, 386-390 (1985).
17. G.L. Closs and O.D. Redwine, *J. Am. Chem. Soc.*, **107**, 4543-454 (1985).
18. A. L. Buchachenko, A.M. Vasserman, *Stable radicals*, Chimia, Moscow, 1973.
19. I.V. Koptuyug, E.G. Bagryanskaya et al., *Chem. Phys. Lett.*, **163**, 503-508 (1989).
20. I.V. Koptuyug, E.G. Bagryanskaya et al., *Chem. Phys. Lett.*, (1990), in press.
21. G.L. Closs., *Advan. Magn. Reson.*, **7**, 154-229 (1974).
22. G.L. Closs and C. E. Doubleday, *J. Am. Chem. Soc.*, **94**, 9248-9249 (1972).
23. E.G. Bagryanskaya, V.F. Tarasov et al., *Chem. Phys. Lett.*, (1990), in press.
24. N. J. Turro, I. R. Gould, B.M. Baretz, *J. Phys. Chem.*, **87**, 531-532 (1983).
25. H. Paul, H. Fisher, *Helvetica Chimia Acta*, **56**, 1575-1580 (1973).
26. Y.A. Kruglak, V.N. Kuprievich, *Dokl. Bolgar. Akad. Nauk.*, **23**, 89-91 (1970).